



Galactic chemical evolution and chemical tagging with open clusters

ARUMALLA B. S. REDDY^{1,*}, SUNETRA GIRIDHAR¹ and DAVID L. LAMBERT²

¹Indian Institute of Astrophysics, Bengaluru 560034, India.

²W.J. McDonald Observatory and Department of Astronomy, The University of Texas at Austin, Austin, TX 78712, USA.

E-mail: balasudhakara.reddy@iiap.res.in

MS received 6 September 2020; accepted 21 October 2020

Abstract. The article presents the consolidated results drawn from the chemical composition studies of Reddy *et al.* (2012, 2013, 2015, 2016) and Reddy & Lambert (2019), who through the high-dispersion echelle spectra ($R = 60000$) of red giant members in a large sample of Galactic open clusters (OCs), derived stellar parameters and chemical abundances for 24 elements by either line equivalent widths or synthetic spectrum analyses. The focus of this article is on the issues with radial-metallicity distribution and the potential chemical tags offered by OCs. Results of these studies confirm the lack of an age–metallicity relation for OCs but argue that such a lack of trend for OCs arise from the limited coverage in metallicity compared to that of field stars which span a wide range in metallicity and age. Results demonstrate that the sample of clusters constituting a steep radial metallicity gradient of slope -0.052 ± 0.011 dex kpc^{-1} at $R_{\text{gc}} < 12$ kpc are younger than 1.5 Gyr and located close to the Galactic midplane ($|z| < 0.5$ kpc). Whereas the clusters describing a shallow slope of -0.015 ± 0.007 dex kpc^{-1} at $R_{\text{gc}} > 12$ kpc are relatively old with a striking spread in age and height above the midplane ($0.5 < |z| < 2.5$ kpc). Results of these studies reveal that OCs and field stars yield consistent radial metallicity gradients if the comparison is limited to samples drawn from the similar vertical heights. The computation of Galactic orbits reveals that the outer disk OCs were actually born inward of 12 kpc but the orbital eccentricity has taken them to present locations very far from their birthplaces. Published results for OCs show that the abundances of the heavy elements La, Ce, Nd and Sm but not so obviously Y and Eu vary from one cluster to another across a sample all having about the solar metallicity. For La, Ce, Nd and Sm the amplitudes of the variations at solar metallicity scale approximately with the main *s*-process contribution to solar system material. Consideration of published abundances of field stars suggest that such a spread in heavy element abundances is present for the thin and thick disk stars of different metallicity. This result provides an opportunity to chemically tag stars by their heavy elements and to reconstruct dissolved open clusters from the field star population.

Keywords. Galaxy: abundances—Galaxy: disk—Galaxy: kinematics and dynamics—(Galaxy:) open clusters and associations: general—stars: abundances.

1. Introduction

The formation and evolution of galaxies in the expanding Universe (far-field cosmology) is one of the major puzzles of astrophysics. The theory of cosmic structure formation based on Lambda Cold

Dark Matter (Λ CDM) models suggests that galaxies form through hierarchical assembly of dark matter halos (Springel *et al.* 2005; Vogelsberger *et al.* 2014). The evolution of baryonic matter confined in each of these halos is expected to construct visible galactic components via star forming process, such as disks and stellar halos as observed in the Milky Way. However, the theoretical models of galaxies are phenomenological models and rely more heavily on the observable properties (e.g., chemical abundances,

This article is part of the Topical Collection: Chemical elements in the Universe: Origin and evolution.

kinematics) of stars than on physical theory. In this regard, the Milky Way Galaxy provides an excellent testing ground for models of galaxy formation and evolution thanks to the ability to resolve individual stars of its stellar populations and analyse them in exquisite detail (Magrini *et al.* 2009; Minchev *et al.* 2013; Kubryk *et al.* 2015). Understanding the assembly history of the Milky Way (near-field cosmology) would help us in unravelling how the formation of individual stellar populations relates to the evolution of galaxies in the early universe and their forms today (far-field cosmology).

Ensembles of stars in the Milky Way are born in dense molecular clouds as OCs and stellar associations, in which stars of different masses bear very similar chemical composition and kinematics of the natal cloud (De Silva *et al.* 2006; Reddy *et al.* 2015; Reddy & Lambert 2019). An OC is a collection of stars with bound by gravity, whereas the stellar association is a loosely bound group of young stars that fails to form a cluster at birth. Stars are slowly lost from a cluster, primarily through internal dynamical effects, and cluster members join the population of Galactic field stars (e.g., isolated single stars and isolated stellar pairs), already supplemented by stars from the unbound stellar associations. A cluster of even 10, 000 solar masses dissolve in less than 2 Gyr by internal dynamical effects and Galactic tidal forces (Lamers & Gieles 2006). In this scenario in which the dispersal of OCs and stellar associations may control Galactic field star populations, one expects that field, association and cluster stars of comparable age would have very similar chemical compositions.

The set of chemical abundances¹ for a given cluster, as first postulated by Freeman and Bland-Hawthorn (2002), is the tag or label identifying stars of common origin even after the spatial information of a cluster's birthplace has vanished. With the dissolution of clusters formed at different times from the chemically distinct molecular clouds, the spread in chemical tags may be found among the field star populations of different ages. This aspect of distinct chemical tags among OCs and, thus, among the field stars is more easily stated than comprehensively tested for OCs and field stars across the full range of elements. This expectation of the feasibility of 'chemical tagging' has motivated the launch of costly large-scale

spectroscopic surveys including APOGEE (Majewski 2016), Gaia-ESO (Gilmore *et al.* 2012) and GALAH (De Silva *et al.* 2015). In spite of astrophysical significance, the chemical tagging as a search technique, to reconstruct the dissolved OCs towards developing a complete picture of the assembly of the Milky Way, has yet to be realized in practice. By chemically tagging stars, we can establish the evolving mass function of star clusters, can investigate chemical-spatial gradients in 3D across the Galaxy, and can detect and isolate the debris of satellite systems dissolved within the indigenous populations of the Milky Way.

Furthermore, reported results by all the previous studies of OCs (Friel *et al.* 2010; Netopil *et al.* 2016) for the age-[Fe/H] and radial-[Fe/H] (and enhanced $[\alpha/\text{Fe}]$ ratios for OCs at $R_{\text{gc}} > 12$ kpc) relations are in contention with those obtained from the field stars (dwarfs and giants; Cheng *et al.* 2012; Hayden *et al.* 2014; Cepheids Luck & Lambert 2011; Lemasle *et al.* 2013) because of consideration of OCs and field stars with different mixtures of stellar ages and from different slices in vertical height ($|z|$) away from the Galactic midplane (Reddy *et al.* 2016): both the field stars and Cepheids suggest a constant steep decline of [Fe/H] over the radial extent 5 to 16 kpc of the Galactic disk, whereas the OCs present a sudden break at $R_{\text{gc}} = 12$ kpc in the constant steep decline of [Fe/H] with increasing R_{gc} and a shallow slope in the range $R_{\text{gc}} = 12-24$ kpc of the Galactic disk.

This disquieting result highlights the need for a uniform analysis of a large sample of young OCs covering the radial extent of the Galaxy to better constrain the observational framework. In spite of astrophysical significance, not many young OCs (ages < 1500 Myr) are subjected to high-resolution spectroscopy and most of them, except those analysed in our previous studies (Reddy *et al.* 2012, 2013, 2015, 2016), have measured abundances for only one or a few heavy elements in the range from La to Eu. Among the 2167 OCs detected in the Milky Way (Dias *et al.* 2002), only about 90 OCs (4%) are subjected to high-resolution spectroscopy ($R > 25,000$). This paper presents the consolidated results of Reddy *et al.* (2012, 2013, 2015, 2016) and Reddy & Lambert (2019), based on the first homogeneous, high-resolution ($R = 60,000$) chemical abundances of 24 elements (Na to Eu) in 86 red giants belonging to 33 Galactic OCs (about 37% of OCs analysed so far with high-resolution spectroscopy) covering the radial extent $R_{\text{gc}} = 7.7$ kpc to 11.3 kpc of the Milky Way.

¹Stellar abundance of an element X is measured relative to the solar abundance and is denoted by $[X/H]$ ($=\log(N_X/N_H) - \log(N_X/N_H)_{\odot}$). Here N_X and N_H are the number densities of X and hydrogen, respectively, in the star and Sun (\odot).

This article is organized as follows: In Section 2 we describe observations, data reduction and radial velocity measurements. Section 3 is devoted to the abundance analysis and Section 4 presents the radial abundance distribution and chemical tags obtained using OCs. Finally, Section 5 provides the conclusions.

2. Observations and data reduction

The sample of red giants in each of the target clusters was extracted from the WEBDA² database and the astrometric and photometric measurements are cross-checked with the SIMBAD³ astronomical database.

High-resolution and high signal-to-noise (S/N) ratio optical spectra of red giants in 33 Galactic OCs were acquired between 1999 February and 2016 November with the Robert G. Tull coude cross-dispersed echelle spectrograph (Tull *et al.* 1995) at the 2.7-m Harlan J. Smith telescope of the McDonald observatory. On all occasions we employed the camera with a 2048×2048 24 μm pixel CCD detector and 52.67 grooves mm⁻¹ echelle grating with exposures centred at 5060 Å in order 69. We secured two to four exposures of cluster giants with each exposure limited to 20–30 min to minimize the influence of cosmic rays and to acquire S/N of above 100.

All the spectra correspond to a resolving power of $R = 60,000$ (5 km s⁻¹) as measured by the FWHM of Th I lines in comparison spectra. The spectrographic setup was stable throughout the night as inferred by the lack of significant systematic shift of Th I lines in comparison spectra ($\lesssim 1$ mÅ) taken at the beginning and end of the night. Our wavelength scale based on the thorium-argon spectra is accurate within a root-mean-square scatter of 3 mÅ. Multiple spectra of a star were combined to acquire a single spectra whose S/N ratios greatly exceed 100 per pixel, permitting reliable estimate of line equivalent widths (EWs) down to the 3 mÅ level. The combined spectra of each star has S/N values over 100 across many echelle orders, but for wavelengths shorter than about 4000 Å the S/N ratio gradually drops and reaches a value of about 15 around 3600 Å region.

The spectrum of each red giant was trimmed, normalized interactively to unity. The radial velocity (RV) was measured from a set of 20 lines with well-defined line cores. The observed RVs were transformed to the heliocentric velocities using the

rvcorrect routine in IRAF⁴. The methods of observations, data reduction and RV measurements are described in depth in Reddy *et al.* (2012, 2013, 2015).

3. Abundance analysis

As the strength of a spectral line is influenced by the physical conditions in the stellar atmosphere and number density of absorbers, it is required to determine the stellar parameters to estimate the chemical abundances. Following the precepts discussed in Reddy *et al.* (2012), we derived the star's effective temperature and surface gravity by substituting the dereddened⁵ optical and 2MASS photometric colors (B-V), (V-K_s) and (J-K_s) and bolometric correction BC_V into the empirical calibrations of Alonso *et al.* (1999). Estimates of BC_V s were made using the Alonso *et al.* (1999) relation connecting the photometric $T_{\text{eff},s}$ and metallicities.

We performed a differential abundance analysis relative to the Sun by running the *abfind* driver of MOOG⁶ adopting the 1D model atmospheres and the iron line equivalent widths (EWs) following the local thermodynamic equilibrium (LTE) abundance analysis technique described in Reddy *et al.* (2015). The line EWs for a selected sample of clean, unblended, isolated and symmetric spectral lines of various atomic/ionic species were measured manually using routines in IRAF while avoiding the wavelength regions affected by telluric contamination and heavy line crowding. We prepared a linelist of 300 absorption lines covering 23 elements from Na-Eu in the spectral range 4450–8850 Å, as described in Reddy *et al.* (2015). The model atmospheres were interpolated linearly from the ATLAS9 model atmosphere grid of Castelli & Kurucz (2003).

The spectroscopic atmospheric parameters (T_{eff} , $\log g$ and ζ_r) were derived by forcing the model-generated iron line EWs to match the observed ones by imposing the conditions of excitation and ionization equilibrium and the independence between the

⁴IRAF is a general purpose software system for the reduction and analysis of astronomical data distributed by NOAO, which is operated by the Association of Universities for Research in Astronomy, Inc. under cooperative agreement with the National Science Foundation.

⁵The adopted interstellar extinctions are $(A_V, A_K, E(V-K), E(J-K)) = (3.1, 0.28, 2.75, 0.54) * E(B-V)$, where $E(B-V)$ is taken from WEBDA.

⁶MOOG was developed and updated by Chris Sneden and originally described in Sneden (1973)

²<http://www.univie.ac.at/webda/>.

³<http://simbad.u-strasbg.fr/simbad/>.

iron abundances and line's reduced EWs. We consider that the excitation equilibrium is satisfied whenever the slope between $\log \epsilon$ (Fe I) and line's lower excitation potential (LEP) was < 0.005 dex/eV and that the ionization equilibrium is satisfied for $|\log \epsilon$ (Fe I) - $\log \epsilon$ (Fe II)| ≤ 0.02 dex. The adopted ξ_t is considered satisfactory when the slope between the Fe abundance from Fe II lines and the line's reduced EWs was almost zero. As all these stellar parameters are interdependent, several iterations are required to extract a suitable model from the grid of stellar atmospheres so that all the spectral lines in observed spectra are readily reproduced. The conditions of the excitation and ionization equilibrium and a check on the ξ_t measured from iron lines have been verified with a suite of Ni, Sc, Ti, V and Cr lines, as described in detail in Reddy *et al.* (2015). Following Reddy *et al.* (2015), typical errors are ± 75 K in T_{eff} , 0.25 cm s $^{-2}$ in $\log g$ and 0.20 km s $^{-1}$ in ξ_t .

The abundance analysis was extended to other species in the linelist using EWs but synthetic profiles were computed for lines affected by hyperfine structure (hfs) and isotopic splitting and/or affected by blends. Our linelists have been tested extensively to reproduce the solar and Arcturus spectra before applying them to selected spectral features in the stellar spectra of program stars. We used a standard synthetic profile fitting procedure by running the *synth* driver of MOOG adopting the spectroscopically determined stellar parameters.

4. Results

The abrupt break at $R_{\text{gc}} = 12$ kpc in the constant steep decline of radial-metallicity distribution of OCs, flattening of the gradient in the outer disk ($R_{\text{gc}} > 12$ kpc), and the enhanced $[\alpha/\text{Fe}]$ ratios of outer Galactic disk OCs have been the subject of many previous studies (Sestito *et al.* 2008; Pancino *et al.* (2010; Friel *et al.* 2010; Yong *et al.* 2012; Cantat-Gaudin *et al.* 2016; Netopil *et al.* 2016). These results from OCs are in contention with those measured for the field stars and Galactic Cepheids: both the field stars and Cepheids suggest a constant steep decline of metallicity over the radial extent 5 to 16 kpc of the Galactic disk, whereas the OCs present a sudden break at $R_{\text{gc}} = 12$ kpc and a shallow gradient in the radial range $R_{\text{gc}} = 12$ –24 kpc (Figures 1 and 2).

To investigate these puzzles, we enlarged the analysed samples of OCs by combining our 33

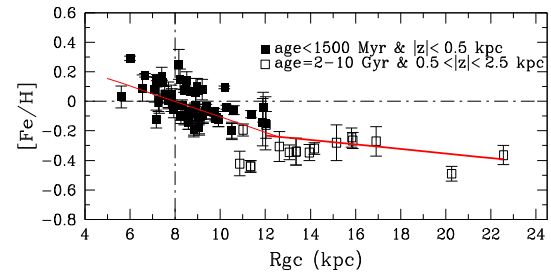


Figure 1. $[\text{Fe}/\text{H}]$ vs. R_{gc} for a sample of Cepheids (Luck & Lambert 2011). A broken line with a slope of -0.062 dex kpc^{-1} represents the fit to the data.

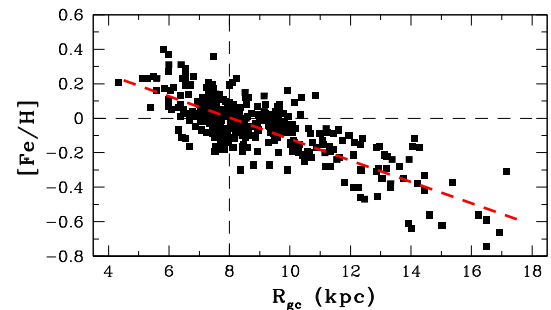


Figure 2. $[\text{Fe}/\text{H}]$ vs. R_{gc} for a sample of Cepheids (Luck and Lambert 2011). A broken line with a slope of -0.062 dex kpc^{-1} represents the fit to the data.

clusters with a sample of 51 OCs in the literature. The systematic errors between the combined samples were removed following a novel approach of adopting the published line EWs of literature sample of cluster stars rather than the published elemental abundances (which are influenced by analysis methods, choice of spectral lines, and type of stellar model grids employed by various authors) of stars/cluster itself (Reddy *et al.* 2015). We have remeasured values of $[\text{Fe}/\text{H}]$, $[\alpha/\text{Fe}]$ and other elements using our linelist (atomic physics data), model atmospheres and reference solar abundances so as to place all results on a common abundance scale and recalculated the cluster's $R_{\text{gc}} =$ to bring all OCs to a common distance scale. We computed the kinematic membership of OCs to either the thin disk, thick disk or halo stellar populations and the cluster's birthplace in the Galaxy (Reddy *et al.* 2016).

This enlarged, homogeneous dataset of OCs provided the first convincing evidence that the sample of clusters constituting a steep radial-metallicity gradient of slope -0.052 ± 0.011 dex kpc^{-1} at $R_{\text{gc}} < 12$ kpc are younger than 1.5 Gyr and located close to the Galactic midplane ($|z| < 0.5$ kpc) with kinematics typical of the thin disk. Whereas the clusters

describing a shallow slope of -0.015 ± 0.007 dex kpc^{-1} at $R_{\text{gc}} > 12$ kpc are relatively old, thick disk members (and hence enhanced in $[\alpha/\text{Fe}]$ ratios) and are away from the Galactic midplane ($0.5 < |z| < 2.5$ kpc). We demonstrated via the computation of birthplaces of OCs that all those OCs located presently at $R_{\text{gc}} > 12$ kpc were actually born inward of 12 kpc but the orbital eccentricity (migration) has taken them to present locations very far from their birthplaces (Reddy *et al.* 2016).

4.1 Chemical tagging

The majority of field stars now in the Galactic disk were born in dense molecular clouds and joined the disk after membership in an OC or an association whose members exhibit internal chemical homogeneity to better than 0.05 dex and bear kinematics of the natal cloud. The set of abundances for a given cluster, as first postulated by Freeman & Bland-Hawthorn (2002), is the tag or label identifying stars of common origin even after the spatial information of a cluster’s birthplace has vanished. In spite of astrophysical significance, the chemical tagging as a search technique has yet to be realized in practice.

The viability of chemical tagging depends on the presence, magnitude and nature of inter-cluster abundance differences. This expectation was searched for in Reddy *et al.* (2015) and Lambert & Reddy (2016) using the young OCs of solar-metallicity which provides a novel result that inter-cluster abundance spread exceeding almost ten times the measurement errors is seen for the heavy *s*-process elements La, Ce, Nd and Sm from AGB-stars (for example, Figure 3). These authors provide a novel result that the spread in heavy elements found among OCs is present but previously unrecognized among local field giants and dwarfs (Lambert and Reddy 2016). This new result by Reddy *et al.* (2015) and Lambert & Reddy (2016) provides an opportunity to chemically tag stars by their heavy elements and to reconstruct dissolved OCs from the field star population.

These observational findings received a measure of support by theoretical considerations by Armillotta *et al.* (2018), who found that elements produced by AGB stars are expected to correlate only when the spatial length scales of star forming regions are lower than 100 parsec, while elements produced by supernovae (Type Ia, Type II SN) and neutron star mergers are significantly correlated even on length scales of

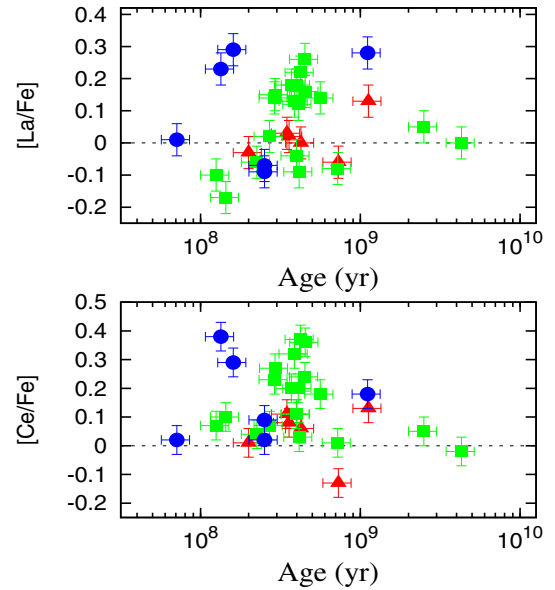


Figure 3. $[X/\text{Fe}]$ versus age (yr) for the heavy elements La and Ce in OCs analysed by Reddy *et al.* (2012, 2013, 2015, 2016) and Reddy & Lambert (2019). Clusters with mean $[\text{Fe}/\text{H}]$ of 0.00 ± 0.05 (6 OCs), -0.10 ± 0.05 (19 OCs) and -0.20 ± 0.05 (6 OCs) are denoted by red triangles, green squares and blue circles, respectively.

1000 pc (i.e., AGB-generated elements are particularly suitable for chemical tagging studies, since their fluctuation scales are comparable with the size of star-forming Giant Molecular Clouds).

5. Conclusion

The aim of the Reddy *et al.* (2012, 2013, 2015, 2016) and Reddy & Lambert (2019) studies of the chemical composition of red giants in OCs is to provide insights into Galactic chemical evolution (GCE). Here, the focus has been on two issues: radial–metallicity distribution and the potential chemical tag offered by heavy element abundances.

First, our homogeneous sample of OCs confirm previous results of a constant steep decline of OC metallicity with increasing R_{gc} of about 12 kpc and a further flattening out to the entire radial extent of the Galactic disk. However, our analysis is the first to demonstrate clearly that such bimodality accompanied by a sudden change in the slope of radial metallicity distribution of OCs at 12 kpc arise from the selection effects; at $R_{\text{gc}} < 12$ kpc the sampled clusters are located close to the Galactic midplane ($|z| < 0.5$ kpc), younger than 1.5 Gyr and constituting a constant steep decline of $[\text{Fe}/\text{H}]$ with R_{gc} while the OCs populating

the disk beyond 12 kpc are older with ages from 1.0 to 8.0 Gyr, metal-poor by $[\text{Fe}/\text{H}] < -0.2$ dex, located away from the Galactic midplane ($0.5 < |z| < 2.5$ kpc) and constitute a shallow gradient over the entire radial extent of the Galactic disk followed by a change of slope at 12 kpc.

Heavy element abundances – Y, La, Ce, Nd, Sm and Eu – for the 33 clusters examined earlier by Reddy *et al.* (2012, 2013, 2015, 2016) and Reddy & Lambert (2019) show that abundances of La, Ce, Nd and Sm with respect to lighter elements (Mg-Ni, for example) may vary by about 0.4 dex. Such abundance variations in heavy elements found for OCs (Reddy *et al.* 2012, 2013, 2015, 2016; Reddy & Lambert 2019; Lambert & Reddy 2016) confirm very similar results provided by Lambert & Reddy (2016) for the literature sample of field dwarfs (Bensby *et al.* 2014; Delgado Mena *et al.* 2017) and giants (Luck 2015). In principle, ratios such as $[\text{La}/\text{Fe}]$ or $[\text{Ce}/\text{Fe}]$ may serve as chemical tags and so identify field stars resulting from a common now-dissolved clusters. This will be very difficult because the run of La, etc., abundances versus $[\text{Fe}/\text{H}]$ (or age) for common Mg-Ni abundances appears continuous at the present precision of the abundances. Perhaps, if the abundance data is combined with kinematical information of the precision now provided by Gaia, chemo-dynamical tagging may be able to connect field stars from a common star-forming complex.

Acknowledgements

We thank the referee for helpful comments. This research has made use of the WEBDA database, operated at the Institute for Astronomy of the University of Vienna and the NASA ADS, USA. This research has made use of “Aladin sky atlas” developed at CDS, Strasbourg Observatory, France. This publication makes use of data products from the Two Micron All Sky Survey, which is a joint project of the University of Massachusetts and the Infrared Processing and Analysis Center/California Institute of Technology, funded by the National Aeronautics and Space Administration (NASA) and the National Science Foundation (NSF).

References

Alonso A., Arribas S., Martínez-Roger C. 1999, A&AS, 140, 261

- Armillotta L., Krumholz M. R., Fujimoto Y. 2018, MNRAS, 481, 5000
- Bensby T., Feltzing S., Oey M. S. 2014, A&A, 562, A71
- Cantat-Gaudin T., Donati P., Vallenari A., Sordo R., Bragaglia A., Magrini L. 2016, A&A, 588, 120
- Castelli F., Kurucz R. L. 2003, IAU Symposium 210, Modelling of Stellar Atmospheres, Uppsala, Sweden, eds. N.E. Piskunov, W.W. Weiss, and D. F. Gray, 2003, ASP-S210
- Cheng J. Y., Rockosi C. M., Morrison H. L. *et al.* 2012, ApJ, 746, 149
- Delgado Mena E., Tsantaki M., Adibekyan V. Zh., Sousa S. G., Santos N. C., González Hernández J. I., Israelian G. 2017, A&A, 606, 94
- De Silva G. M., Freeman K. C., Bland-Hawthorn J., *et al.* 2015, MNRAS, 449, 2604
- De Silva G. M., Sneden C., Paulson D. B. *et al.* 2006, AJ, 131, 455
- Dias W. S., Alessi B. S., Moitinho A., Lépine J. R. D. 2002, A&A, 389, 871
- Freeman K., Bland-Hawthorn J. 2002, ARA&A, 40, 4875
- Friel E. D., Jacobson H. R., & Pilachowski C. A. 2010, AJ, 139, 1942
- Gilmore G., Randich S., Asplund M. *et al.* 2012, The Messenger, 147, 25
- Hayden M. R., Holtzman J. A., Bovy J. *et al.* 2014, AJ, 147, 116
- Kubryk M., Prantzos N., Athanassoula E. 2015, A&A, 580, 126
- Lambert D. L., Reddy A. B. S. 2016, ApJ, 831, 202
- Lamers H. J. G. L. M., Gieles M. 2006, A&A, 455, 17
- Lemasle B., François P., Genovali K. *et al.* 2013, A&A, 558, 31
- Luck R. E. 2015, AJ, 150, 88
- Luck R. E., Lambert D. L. 2011, AJ, 142, 136
- Magrini L., Sestito P., Randich S., Galli D. 2009, A&A, 494, 95
- Majewski S. R. 2016 APOGEE Team, APOGEE-2 Team, AN, 337, 863
- Minchev I., Chiappini C., Martig M. 2013, A&A, 558, 9
- Netopil M., Paunzen E., Heiter U., Soubiran C. 2016, A&A, 585, 150
- Pancino E., Carrera R., Rossetti E., Gallart C. 2010, A&A, 511, A56
- Reddy A. B. S., Giridhar S., Lambert D. L. 2015, MNRAS, 450, 4301
- Reddy A. B. S., Giridhar S., Lambert D. L. 2013, MNRAS, 431, 3338
- Reddy A. B. S., Giridhar S., Lambert D. L. 2012, MNRAS, 419, 1350
- Reddy A. B. S., Lambert D. L. 2019, MNRAS, 485, 3623
- Reddy A. B. S., Lambert D. L., Giridhar S. 2016, MNRAS, 463, 4366

- Sestito P., Bragaglia A., Randich S., Pallavicini R., Andrievsky S. M., Korotin S. A. 2008, *A&A*, 488, 943
- Sneden C., 1973, PhD Thesis, Univ. of Texas, Austin
- Springel V., White S. D. M., Jenkins A. *et al.* 2005, *Nature*, 435, 629
- Tull R.G., MacQueen P.J., Sneden C., Lambert D.L. 1995, *PASP*, 107, 251
- Vogelsberger M., Genel S., Springel V. *et al.* 2014, *MNRAS*, 444, 1518
- Yong D., Carney B. W., Friel E. D. 2012, *AJ*, 144, 95